Acta Cryst. (1952). **5**, 615

The Use of the Three-Stage Electron Microscope in Crystal-Structure Analysis

BY J. F. BROWN AND D. CLARK

Research Department, Imperial Chemical Industries Limited, Billingham, Co. Durham, England

(*Received* 15 *December* 1951 *and in revised form* 14 *January* 1952)

The combination of electron diffraction and electron microscopy in a three-stage electron microscope enables electron-diffraction patterns to be obtained from extremely small single crystals, i.e. less than 1μ across and 1000 Å thick. Two examples are described in which it is shown how these single-crystal diffraction patterns can be used to obtain valuable crystallographic information concerning unit-cell size and symmetry. Thus the unit cell of the σ phase from a Cr–Ni–Mo steel was shown by electron-diffraction patterns from a micro-crystal to be tetragonal with $a = 8{\cdot}8$, $c = 4{\cdot}5$ Å. The experimental difficulties and limitations are discussed and the usefulness of the method as an addition to the normal diffraction techniques for crystal-structure analysis is demonstrated, particularly in cases where the only X-ray data available are a powder photograph.

Introduction

It is the purpose of this paper to discuss the application of electron diffraction to unsolved structure problems, particularly in those cases where X-rays methods by themselves have failed. The determination of unit-cell size and symmetry from X-ray photographs of single crystals is a routine matter but the extraction of such information from photographs of powders and polycrystalline aggregates is a problem which becomes progressively more difficult as the symmetry of the unit cell decreases and the size increases. Although a number of analytical procedures have been described, e.g. by Ito (1950) they are by no means completely satisfactory or unambiguous. The polycrystalline aggregate or powder, however, consists ultimately of single crystals ranging in size from 50 Å, for finely dispersed sols, upwards. If examined under a sufficiently high magnification, the individual crystals comprising the powder may be seen and often show the characteristic straight edges and regular angles of macroscopic crystals. A size range from 50 Å up to about 10μ can be conveniently covered in an electron microscope and various methods have been adopted whereby it is possible to obtain the electron-diffraction pattern corresponding to any chosen part of the visual field. With a suitable preparation, the chosen part of the field may be a single crystal, say, $\frac{1}{2}\mu$ across, in which case a single-crystal electron-diffraction pattern is obtained similar in every way to that obtained from a macroscopic crystal in a conventional electron-diffraction apparatus.

Various techniques have been proposed for electron diffraction from selected specimen areas. Boersch (1940) has used a fine collimated electron beam with a fine aperture and a method using an auxiliary lens has been suggested by Ardenne (1941). Hillier & Davidson (1947) have used a double-lens electron-diffraction camera whereby electron shadow micrographs and electron-diffraction patterns can be obtained. However, the three-stage electron microscope can give diffraction patterns from selected specimen areas with great ease and was used in the investigation described in this paper.

In the following section a brief description is given of the electron optics of a three-stage instrument and the limitations of specimen preparation and technique are pointed out. Then follows an account of work carried out on σ phase and carbide residues obtained from stainless steels which illustrate very well the possibilities of the technique.

Diffraction in a three-stage electron microscope

The optics of a three-stage microscope have already been fully described by Challice (1950). The change-over from ordinary image to diffraction is accomplished merely by altering the focal length of the intermediate lens by changing the current through the field coils. The change is shown diagrammatically in Figs. 1 and 2. Fig. 1 shows ordinary image formation at high magnification, e.g. 5000×. Fig. 2 shows the state of affairs when the strength of the intermediate lens has been reduced so that it now images the back focal plane of the objective lens, where, according to Abbé, a diffraction pattern of the specimen is formed. The image of this pattern formed by the intermediate lens is then magnified by the projector lens and can be seen on the final fluorescent screen. A diffraction aperture can be inserted in the image plane of the objective lens so that it excludes all rays except those coming from the selected field. The final diffraction pattern is therefore from this field alone. The size of the diffraction aperture is such that it limits the specimen field to a diameter of only a few microns. In a normal three-stage instrument the size of the diffraction pattern is of the same order as that obtained in a

conventional apparatus, with a camera length of 50 cm. When the field contains very many small crystals, the diffraction pattern is the well-known polycrystalline ring pattern analogous to an X-ray powder pattern and no more amenable to interpretation. If, however, the field contains a single-crystal flake 100–1000 Å thick and a few square microns in area, single-crystal spot patterns are obtained.

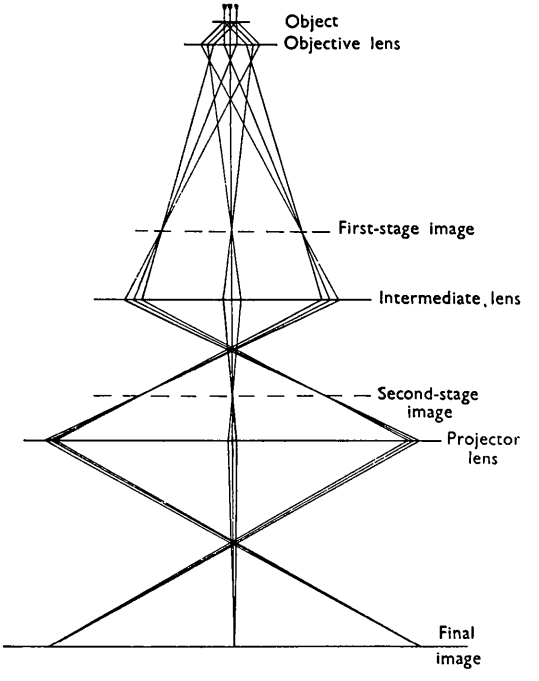

Fig. 1. Ray diagram showing image formation at high magnification.

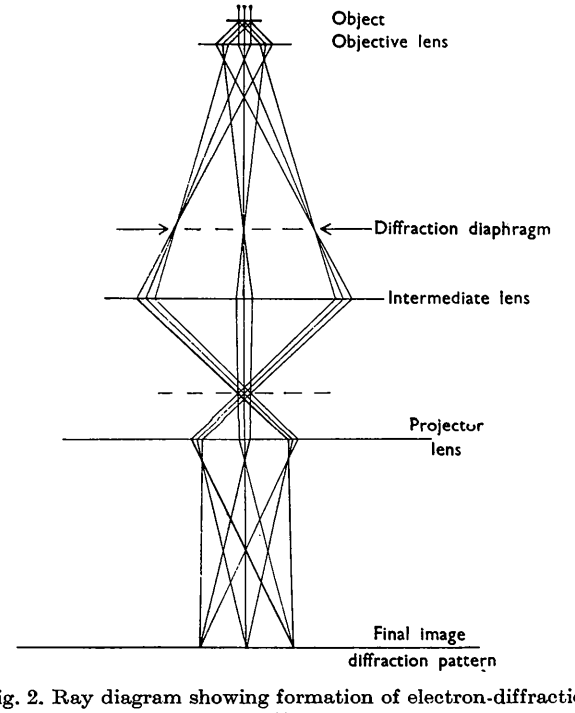

Fig. 2. Ray diagram showing formation of electron-diffraction pattern.

To interpret the spot pattern it is necessary to know the effective camera length L, and the accelerating voltage from which the wavelength λ of the electron beam can be determined. The camera length L cannot, of course, be directly measured since it depends on the magnification of the lens and the specimen position. Calibration with a known substance under fixed experimental conditions gives the camera constant λL which is adequate for the interpretation of polycrystalline ring patterns. However, in single-crystal work, a knowledge of the separate values λ and L is essential. These can only be determined indirectly so that the accuracy of spacings derived from spot patterns is limited.

A more serious difficulty than experimental inaccuracy is that the orientation of the specimen with respect to the electron beam is unknown and fixed by the fortuitous angle of the crystal with regard to the specimen-supporting grid. In some types of microscope the specimen holder can be rotated about one axis by 5–10°, but this, in general, is insufficient to alter materially the diffraction pattern. In practice this is not an insuperable difficulty since the type of crystal most suitable for electron diffraction is a thin flake which naturally lies flat on the supporting film perpendicular to the beam direction. Moreover the 'thin' direction is usually a prominent crystallographic direction so that in most cases in which a good single-crystal pattern is obtained a prominent crystallographic direction is approximately parallel to the beam direction.

Interpretation of single-crystal patterns

The interpretation of single-crystal patterns has been well described in the literature. Finch & Wilman (1937) have described the patterns from single crystals and Charlesby, Finch & Wilman (1939) showed how the electron-diffraction method could be applied to the study of the crystal structure of anthracene, whilst Wilman (1948) has described in detail the interpretation of Kikuchi-line patterns.

However, in the three-stage microscope the single-crystal patterns are usually single cross-grating spot patterns due to the intersection of the nearly straight and equidistant Laue zones from two important lattice rows approximately perpendicular to the incident beam, the intensities being modified by the circular Laue zones associated with the third lattice row approximately parallel to the beam direction. The effective length of the lattice rows perpendicular to the beam will usually exceed 1000 Å and the Laue zones from these rows approximate, therefore, to straight lines, which intersect in a series of sharp spots. The third lattice row, parallel to the beam, is, however, of limited length if the crystal is sufficiently thin to diffract, and the circular Laue zones are therefore

always somewhat broad. In the extreme case when the thickness of the crystal is less than 200 Å the zones are so broad that they completely overlap and the resultant pattern approximates to that of a two dimensional cross grating. An alternative approach is via the reciprocal lattice with the lattice points extended in the 'thin' direction of the crystal. In either case it is possible to determine the spacings of two important lattice rows and the angle between them, and often a third row approximately perpendicular to the other two. In favourable cases this is sufficient to establish the size and shape of the unit cell within limits sufficiently close to provide a sound starting point for indexing the low-angle reflexions of complex powder photographs. The X-ray spacings, thus indexed with a reasonable degree of certainty, can then be used to provide somewhat more accurate unit cell parameters, the process of refinement being continued in the usual way until accurate parameters have been obtained from high angle reflexions. The experimental uncertainties of the electron-diffraction measurements are such that it is not possible to distinguish between, say, tetragonal and orthorhombic cells with two axes almost equal, or between orthogonal axes and axes departing slightly from 90°. In such cases, it seems reasonable to assume the highest symmetry until it is apparent that the multiplicity of reflexions on the X-ray powder pattern cannot be explained on such a basis. Trial-and-error methods must then be used to determine the exact distortion required to account for the observed X-ray data. In the case of the σ phase studied here, no degradation of the postulated symmetry was required. There seems no doubt, however, that, even in less symmetrical cases, the information given by single-crystal electron diffraction photographs would be an extremely valuable guide to the application of strictly analytical procedures of the type proposed by Ito.

Electron-diffraction investigation of chrome nickel steels

The conventional methods of investigating the behaviour of alloy systems are (*a*) by microscopy, including electron microscopy to an ever increasing extent, (*b*) X-ray investigations, usually by powder methods. We have investigated two alloy steels 18% Cr/8% Ni/2% Mo/1% Ti and 25% Cr/20% Ni after heat treatment in the temperature range 650–850° C. for periods up to 1000 hr. with particular emphasis on the growth of σ phase—a brittle intermetallic compound of ideal composition FeCr—and on the precipitation of carbides. It would be out of place here to describe in detail the metallurgical aspects of the work. X-ray results showed a σ phase to be formed in both series and at the same time showed that the carbide precipitated was $Cr_{23}C_6$. The X-ray powder photograph of the σ phase (Fig. 3) is well known, the main features being the group of strong reflexions around 2·0 Å, and other groups at higher angles. Owing to the complete absence of reflexions corresponding to large spacings it has proved impossible to interpret the pattern on any logical basis although a number of unit cells have been postulated in the literature based on agreement between observed and calculated spacings (Pietrokowsky & Duwez, 1950).

The crystal habit of the phase differs markedly in the two alloys studied. Surface replicas from polished micro-sections showed that in 25/20 alloy the characteristic form is needles growing in the austenite matrix (Fig. 4) which, on prolonged heat treatment in the temperature range studied, grow into the more massive forms shown in Fig. 5. In 18/8 steel, however, the habit is thin plates resulting from the complete breakdown of the original ferrite grains to give characteristic islands of σ (Fig. 6).

By a process of electrolytic extraction in 4% HCl aq. and current density of 0·5 A.cm.$^{-2}$, it is possible to dissolve away the austenite matrix leaving an insoluble sludge of σ phase and chromium carbide. After washing and drying, this fine powder can be examined directly in the microscope. The shapes of the individual particles (Figs. 7 and 8) may easily be correlated with the characteristic forms shown in the replicas. At the outset of the investigation it was hoped that sufficiently large crystals could be obtained by prolonged heat treatment to enable a single-crystal X-ray investigation to be carried out. It was soon apparent that suitable crystals were not readily obtainable but the possibility of obtaining electron-diffraction patterns from micro-crystals suggested itself as a promising alternative. The best results were obtained using a Philips microscope operating at 100 kV. in which the large field of view is a distinct advantage for showing up the circular Laue zones. The needles obtained from 25/20 steels were not ideal and gave rather poor diffraction patterns not readily amenable to direct interpretation. The thin flakes from heat-treated 18/8 steels were much more promising, and gave excellent single-crystal patterns (Fig. 10) with well-defined Laue zones. The simplest and most common pattern was an approximately square cross grating superimposed on Laue zones due to the lattice row in the beam direction. From this pattern can be deduced cell dimensions 8·8 Å×8·8 Å×4·5 Å; a tetragonal unit cell with the fourfold axis approximately parallel to the beam direction. Using these approximate dimensions it is possible, without too much difficulty, to assign indices to all the reflexions in the first strong group of the X-ray powder photographs. From these indexed reflexions more accurate values of cell dimensions are obtained and the whole pattern can be indexed very rapidly by successive approximations. No unexplained reflexions remain so that it is not necessary to reduce the symmetry of the unit cell below tetragonal. The final cell parameters are

$$a = 8{\cdot}809 \pm 0{\cdot}004,\ c = 4{\cdot}585 \pm 0{\cdot}002\ \text{Å}.$$

Fig. 3. X-ray powder pattern of σ phase from 18/8/Mo/Ti steel. 19 cm. camera. Co $K\alpha$ radiation.

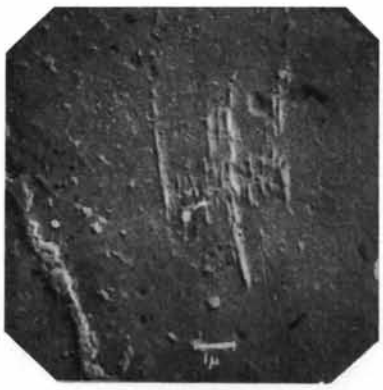

Fig. 4. Electron micrograph of shadowed surface replica from 25/20 steel after heat treatment for 4 hr. at 750° C. Magnification 5000×.

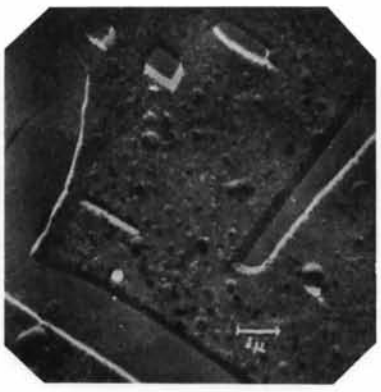

Fig. 5. Electron micrograph of shadowed surface replica from 25/20 steel after heat treatment for 1000 hr. at 950° C. Magnification 5000×.

Fig. 6. Electron micrograph of shadowed surface replica from 18/8/Mo/Ti steel after heat treatment for 24 hr. at 850° C. Magnification 2500×.

Fig. 7. Electron micrograph of needles of σ phase extracted electrolytically from heat-treated 25/20 steel. Magnification 5000×.

Fig. 8. Electron micrograph of single-crystal flake extracted electrolytically from heat-treated 18/8/Mo/Ti steel. Magnification 2500×.

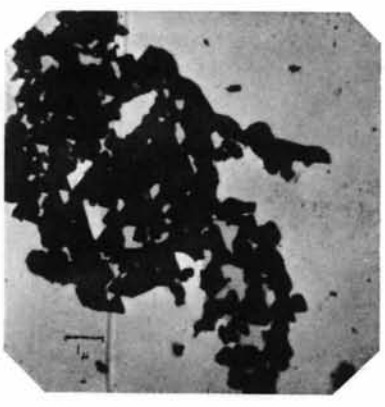

Fig. 9. Electron micrograph of crystal of chromium carbide, $Cr_{23}C_6$, extracted from 25/20 steel. Magnification 5000×.

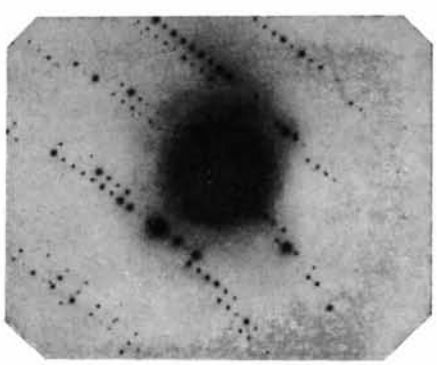

Fig. 10. Electron-diffraction pattern from single-crystal flake of σ phase from 18/8/Mo/Ti steel.

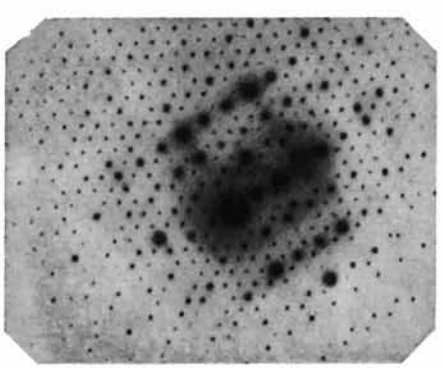

Fig. 11. Electron-diffraction pattern from single crystal of chromium carbide, $Cr_{23}C_6$, extracted from 25/20 steel. Magnification 5000×.

[*To face p.* 617

Table 1 shows the very satisfactory agreement between observed and calculated spacings. A striking feature is the absence of low-order reflexions on the powder

Table 1. 18/8 Mo/Ti σ *phase*

19 cm. camera. Co $K\alpha$ radiation
$a = 8{\cdot}809 \pm 0{\cdot}004$, $c = 4{\cdot}585 \pm 0{\cdot}002$ Å

I_o	d_c (Å)	d_c (Å)	(*hkl*)
vvvw	2·574	2·576	221
mw−	2·3807	2·380	311
m+	2·2931	2·293	002
s	2·1354	2·135	410
m+	2·0763	2·077	330
ms	2·0328	2·033	202
s+	1·9810	1·981	122
vs	1·9358	1·936	411
s	1·8912	1·891	331
m−	1·8452	1·846	222
m−	1·7686	1·769	312
vvvw	1·6729	1·671	322
vvvw	1·6410	1·644	501
vvvw	1·6161	1·616	511
w−	1·3964	1·396	432
w	1·3799	1·380	611
mw	1·3305	1·332	621
		1·331	522
m	1·2612	1·262	631
		1·261	532
s	1·2431	1·245	550
		1·243	413
mw	1·2366	1·236	602
m−	1·2305	1·230	333
mw	1·2240	1·224	612
m	1·2100	1·209	720
w+	1·2015	1·200	551
			711
w	1·1901	1·190	622
w	1·1787	1·180	641
m−	1·1694	1·168	721
m+	1·1460	1·146	004
m	1·0678	1·068	820
m−	1·0405	1·040	821
m	1·0385	1·038	660
s	1·0100	1·010	414
m+	1·0034	1·003	334
mw	0·9919	0·992	642
ms	0·9858	0·9858	812
		0·9837	840

pattern which would give a clue as to the size of the rather large unit cell. This explains the difficulty of indexing the pattern by analytical methods in spite of the relatively high symmetry of the unit cell.

Other electron-diffraction patterns were obtained from crystals in other orientations and of different habits, but these were not fully worked out since, while the investigation was in progress, it was learned that the structure had been solved by X-ray methods using single crystals of pure FeCr σ phase. The dimensions of the tetragonal unit cell were given as $a = 8{\cdot}79$, $c = 4{\cdot}55$ Å. Our results from powder photographs of a molybdenum-bearing alloy are therefore in excellent agreement with determinations from single crystals (Dickens, Douglas & Taylor, 1951; Shoemaker & Bergman, 1950).

Crystal habit of chromium carbide, $Cr_{23}C_6$

During the examination of electrolytic extracts from the 25/20 series, interesting results were obtained on the crystal growth of $Cr_{23}C_6$, a preliminary account of which has already been given (Brown & Clark, 1951). It was found from an electron microscope examination that the carbide first appears as flakes which grow, on continued heat treatment, into masses of interconnected equilateral triangles all in perfect orientation (Fig. 9). All these structures give excellent single-crystal electron-diffraction patterns (Fig. 11). The pattern is a regular hexagonal cross grating with a spacing of 7·5 Å, with superposed circular Laue zones due to a repeat distance of about 20 Å roughly parallel to the beam direction. Chromium carbide is face-centred cubic $a = 10{\cdot}68$ Å and will give a hexagonal cross grating pattern with a (111) plane perpendicular to the beam direction. The hexagonal translation is $a/\sqrt{2} = 7{\cdot}5$ Å and the repeat distance in the [111] direction $a\sqrt{3} = 18{\cdot}5$ Å. There is thus conclusive proof of the identity of the triangular structure with $Cr_{23}C_6$, thus confirming the work of Mahla & Nielsen (1951) who, from electron micrographs alone, concluded that the growth of this carbide is governed by (111) planes of the matrix.

Conclusion

These two examples described in detail show how the unique combination of electron diffraction and electron microscopy in a single instrument can be used to obtain valuable crystallographic information concerning unit-cell size and symmetry when the only crystals available are extremely small, 1μ across and 500 Å thick. It is not claimed that complete structure analyses are possible but the information is such as to make possible the more ready interpretation of X-ray powder photographs which, for microcrystalline substances, represent the only X-ray data available.

The difficulties of obtaining accurate lattice spacings are described but these could be overcome without great trouble. Furthermore, some form of stage allowing rotational movement of the specimen about two axes normal to the beam direction would greatly assist in obtaining patterns with suitable specimen orientations. Even with the experimental difficulties and the limitation of the type of specimen, the method should be a useful addition to the X-ray diffraction techniques for crystal-structure analysis.

References

Ardenne, M. von (1941). *Z. Phys.* **117**, 515.

Boersch, H. (1940). *Z. Phys.* **116**, 469.

Brown, J. & Clark, D. (1951). *Nature, Lond.* **167**, 728.

Challice, C. (1950). *Proc. Phys. Soc.* B, **63**, 59.

Charlesby, A., Finch, G. I. & Wilman, H. (1939). *Proc. Phys. Soc.* **51**, 479.

Dickens, D., Douglas, A. & Taylor, W. H. (1951). *Nature, Lond.* **167**, 192.

FINCH, G. I. & WILMAN, H. (1937). *Ergebn. exakt. Naturw.* **16**, 353.
HILLIER, J. & DAVIDSON, N. (1947). *J. Appl. Phys.* **18**, 499.
ITO, T. (1950). *Nature, Lond.* **164**, 755.
MAHLA, E. M. & NIELSEN, N. A. (1951). *Trans. Amer. Soc. Met.* **43**, 290.
PIETROKOWSKY, P. & DUWEZ, P. (1950). *Trans. Amer. Inst. Min. (Metall.) Engrs.* **188**, 1283.
SHOEMAKER, D. P. & BERGMAN, B. (1950). *J. Amer. Chem. Soc.* **72**, 5793.
WILMAN, H. (1948). *Proc. Phys. Soc.* **60**, 341.

Acta Cryst. (1952). **5**, 619

Die Energieströmung bei Röntgenstrahl-Interferenzen in Kristallen

VON M. v. LAUE

Kaiser-Wilhelm-Institut für physikalische Chemie und Elektrochemie, Faradayweg 4–6, Berlin-Dahlem, Deutschland

Eingegangen am 31. *Januar* 1952)

It is shown how the dynamical theory of X-ray diffraction accounts for the experimentally observed path of the X-ray energy through thick crystals set at reflecting positions. This path is determined only by the nature of the crystal and the wavelength of the X-rays, and is due to the anomalous absorption of the X-rays incident at the Bragg angle.

1. Einleitung

In Übereinstimmung mit den meisten Versuchsanordnungen betrachtet die Theorie der Röntgenstrahlinterferenzen die Breite einer auf den Kristall treffenden Welle im allgemeinen als gross gegen dessen Dicke und fragt nicht nach der seitlichen Begrenzung, also auch nicht nach der Lage der Austrittsstelle zur Eintrittsstelle. Klare Beobachtungen darüber finden sich zuerst wohl bei Cork (1932) und bei Murdock (1934), welche aus einer Dreiteilung von Interferenzpunkten auf eine Dreiteilung der Austrittsstelle schlossen. Später veröffentlichten Du Mond & Bollmann (1936*a*, *b*; 1938), sowie Hirsch (1938), Ähnliches; neuerdings ist Barraud (1951) auf diese Erscheinung zurückgekommen. § 6 wird in Übereinstimmung mit diesen Autoren zeigen, dass es sich dabei zum Teil um Oberflächenerscheinungen handelt. In voller Reinheit hat den Energiestrom durch das Innere erst Borrmann (1950, 1951) gesehen; er liegt, wie auch schon die ältere Literatur angibt, jedenfalls sehr nahe der bei der Interferenz 'spiegelnden' Netzebene. Für nichtabsorbierende Kristalle lässt sich nach §§ 2 und 3 nicht verstehen, dass ein eindeutig angebbarer, von den besonderen Versuchsbedingungen unabhängiger Energieweg zur Beobachtung kommt. Nach § 4 hingegen ist dies die notwendige Folge der Absorption, und zwar jener anomalen Absorption, welche Borrmann (1941, 1950) für den Interferenzfall experimentell entdeckt und der Verfasser in einer früheren Arbeit, welche wir hier als 'I' zitieren (Laue, 1949), dynamisch erklärt hat.

Wie in I setzen wir im Folgenden voraus, dass der abgebeugte Strahl auf der Rückseite der Kristallplatte austritt. Wir übernehmen alle Gleichungen und Bezeichnungen der Veröffentlichung I, benutzen ausserdem Gleichungen aus der 2.-ten Auflage meines Buchs über *Röntgenstrahl-Interferenzen* (Laue, 1948), welche wir als 'II' zitieren; dies benutzt dieselben Bezeichnungen mit der einzigen Ausnahme, dass der Abbeugungswinkel in I und hier 2θ, in II θ genannt ist.

Jede Theorie der Energieströmung in einem elektromagnetischen Felde muss vom Poyntingschen Vektor ausgehen; bei periodischen Schwingungsvorgängen bestimmt dessen Zeit-Mittel über eine Periode den Strahl. Bei Schwingungen im Raumgitter variiert dieses aber noch innerhalb jeder Zelle periodisch nach Grösse und Richtung; daher muss man, um die Strahl-Richtung zu finden, noch eine räumliche Mittelung über die Zelle vornehmen. Das ist der einzige Unterschied gegenüber den sonstigen optischen Problemen.

2. Das einzelne Wellenfeld im nichtabsorbierenden Kristall

Das einfachste elektromagnetische Feld im Raumgitter ist ein aus unendlich vielen ebenen Wellen zusammengesetztes Wellenfeld. Man beschreibt es unter Zugrundelegung der elektrischen Verschiebung $\mathfrak{D}$ durch die Formel*:

$$\mathfrak{D} = \exp[2\pi i\nu t]\,\mathbf{S}_m\mathfrak{D}_m \exp[-2\pi i(\mathfrak{K}_m\mathfrak{r})] \qquad (1)$$

oder, bei Bevorzugung der magnetischen Feldstärke $\mathfrak{H}$, durch die gleichwertige Formel:

$$\mathfrak{H} = \exp[2\pi i\nu t]\,\mathbf{S}_m\mathfrak{H}_m \exp[-2\pi i(\mathfrak{K}_m\mathfrak{r})]\,. \qquad (2)$$

Die Summation nach m bedeutet dreifache Summation

* Die Gleichungen (1), (2), (3) und (4) stehen in II unter den Nummern (26.25), (26.34), (26.24), und (26.35).